Journal of Alloys and Compounds 509 (2011) 9776–9781

Contents lists available at ScienceDirect

Journal of Alloys and Compounds

journal homepage: www.elsevier.com/locate/jallcom

Phase equilibria of the Cu–Ni–Si system at 700 °C

Weihua Sun[a,b], Honghui Xu[a,b,*], Shuhong Liu[a,b], Yong Du[a,b], Zhaohui Yuan[a], Baiyun Huang[a]

[a] State Key Laboratory of Powder Metallurgy, Central South University, Changsha, Hunan 410083, PR China
[b] Science Center for Phase Diagrams & Materials Design and Manufacture, Central South University, Changsha, Hunan 410083, PR China

ARTICLE INFO

Article history:
Received 7 March 2011
Received in revised form 7 July 2011
Accepted 30 July 2011
Available online 4 August 2011

Keywords:
Cu–Ni–Si system
Phase diagram
X-ray diffraction
Electron probe microanalysis

ABSTRACT

The phase equilibria at the isothermal section of the Cu–Ni–Si system at 700 °C were experimentally investigated. Thirty Cu–Ni–Si alloys were prepared by arc melting and annealed at 700 °C for 30 or 80 days, and examined with optical microscopy, X-ray diffraction, scanning electron microscopy with energy dispersive X-ray spectroscopy and electron probe microanalysis. Twelve three-phase regions were determined. The existence of the ternary compound τ_1-$Cu_{56.8-63}Ni_{10.4-16.1}Si_{26.6-27.3}$ reported in literature was confirmed and a new compound τ_2-$Cu_{45.8}Ni_{25}Si_{29.2}$ with nearly no homogeneity range was observed. The θ-Ni_2Si compound, which exists above 820 °C in the binary Ni–Si system, was found to be stable at 700 °C and the composition range of Cu is 12.7–20.6 at.% Cu. The ternary solubilities of binary compounds were measured and noticeably the $Cu_{56}Si_{11}$ compound can dissolve Ni up to 21.9 at.%.

1. Introduction

The Cu–Ni–Si system is an important system in industry. Typically, the Corson alloys (Cu rich, Cu–Ni–Si–$X_{(x=none\ or\ Mg,\ Sn,\ Zn,\ et\ al.)}$ alloy) attracted much attention due to their good balance of high strength, high electrical conductivity and bending formability [1–7]. For example, the Corson alloys C7025 ($Cu_{96.2}Ni_3Si_{0.65}Mg_{0.15}$, in wt.%) with high efficiency are widely used for connectors, lead frames and CPU sockets [8]. NKC164E ($Cu_{98.05}Ni_{1.6}Si_{0.35}$, in wt.%) alloy with high electric conductivity can be used for connectors and wire harness [8]. These Corson alloys feature the age-hardening effect by precipitation of low-temperature Ni_2Si (δ-Ni_2Si) particles or other compounds during heat treatment between 450 °C and 550 °C [9–11]. In addition, the silicon Monel alloys ($Ni_{62-68}Cu_{28-31}Si_{3.5-4.5}Fe_{<3}Mn_{0.5-1.5}$, in wt.%) are used for machine parts subjected to friction and operated under special conditions because of their high strength, ductility, corrosion resistance and wear resistance [12]. Knowledge of the phase equilibria on the Cu–Ni–Si system is very significant for development of advanced Cu–Ni–Si alloy. However, information on the phase equilibria of Cu–Ni–Si is very limited.

The Cu–Ni–Si system has been assessed by Jänecke [13], Chang et al. [14] and Drits et al. [15]. Recently, Hari Kumar et al. [16] made a critical review of the phase equilibria [1–4,17–30] and thermodynamic properties [31] up to the year 2002. He pointed out that there was a great disagreement among the literature data. The significant discrepancies lie in the solubility of the binary compounds, the solubility of the Fcc_A1 phase in the Cu rich corner, the existence and stability of ternary compounds and so on. In the following, the phase diagram data are briefly reviewed with emphasis on the data concerning the present experiment. More information was published by Hari Kumar et al. [16]. By means of thermal analysis (TA), metallographic, X-ray diffraction (XRD), dilatometry and hardness measurement, Okamoto [20–23] investigated and reported several isothermal sections in the Cu-rich corner and many vertical sections. A ternary compound τ with 12–15 wt.% Si and 11–12 wt.% Ni was reported [22]. This ternary compound is formed by the ternary peritectic reaction Liquid + $Cu_{56}Si_{11}$ + θ-$Ni_2Si \leftrightarrow \tau$ at 859 °C and can be stable down to 450 °C. Large solubilities of θ-Ni_2Si (20 wt.%), $Ni_{31}Si_{12}$ (35 wt.%), and $Cu_{56}Si_{11}$ (25 wt.%) were reported [21,22]. Lashko and Sorokina [26] reported several phase equilibria observed in the Cu–Ni side by examining several alloys and found the solubilities of Ni_3Si, $Ni_{31}Si_{12}$ and δ-Ni_2Si are small. Sokolovskaya et al. [27,28] measured the isothermal sections at 500 °C. The ternary compound τ found by Okamoto [22] was not observed. The θ-Ni_2Si phase, which is stable above 820 °C in the binary Ni–Si phase diagram, was observed at 500 °C in the ternary system and it can dissolve 10 at.% Cu.

The experimental binary phase diagrams were compiled in Ref. [32]. Table 1 shows the crystallographic data of the phases at 700 °C in the Cu–Ni–Si system. In the Ni–Si system, Ni_3Si and Ni_3Si_2 show narrow homogeneity. Only $Cu_{15}Si_4$ has no homogeneity in

* Corresponding author at: State Key Laboratory of Powder Metallurgy, Central South University, Changsha, Hunan 410083, PR China. Tel.: +86 731 88877300; fax: +86 731 88710855.
E-mail address: honghuixu08@gmail.com (H. Xu).

0925-8388/$ – see front matter © 2011 Elsevier B.V. All rights reserved.
doi:10.1016/j.jallcom.2011.07.106

Table 1
List of the crystallographic data of the phases at 700 °C in the Cu–Ni–Si system.

Phase	Pearson symbol	Space group	Prototype	Lattice parameters (Å)			Reference
				a/α[a]	b/β[a]	c/γ[a]	
Liquid	–	–	–	–	–	–	–
Fcc_A1	cF4	Fm-3m	Cu	3.615(Cu) 3.5238(Ni)			[33]
Si	cF8	Fd-3m	C	5.4309			[34]
Ni_3Si	cP4	Pm-3m	$AuCu_3$	3.506			[35]
$Ni_{31}Si_{12}$	hP43	P321	$Ni_{31}Si_{12}$	6.667		12.277/120°	[36]
δ-Ni_2Si	oP12	Pbnm	Co_2Si	7.0649	5.0012	3.7307	[37]
Ni_3Si_2	oC80	$Cmc2_1$	Ni_3Si_2	12.229	10.805	6.924	[38]
θ-Ni_2Si[b]	hP4.5	$P6_3/mmc$	Ni_2In	3.855		4.952/120°	[39]
NiSi	oP8	Pnma	MnP	5.18	3.34	5.62	[40]
$NiSi_2$	cF12	Fm-3m	CaF_2	5.395			[41]
Cu_7Si[c]	hP2	$P6_3/mmc$	Mg	2.561		4.184/120°	[37]
$Cu_{56}Si_{11}$[d]	cP19.98	$P4_132$	βMn	6.222			[42]
$Cu_{15}Si_4$	cI76	I-43d	$Cu_{15}Si_4$	9.714			[43]
$Cu_{19}Si_6$	oP16	P	–	6.041	6.356	4.288	[37]

[a] The degrees of the missing α, β, and γ angle are 90°.
[b] The composition is $Cu_{0.15}Ni_{0.5}Si_{0.35}$.
[c] The composition is $Cu_{6.69}Si$.
[d] The composition is $Cu_{83.3}Si_{16.7}$.

the Cu–Si system. The present work is intended to measure the isothermal section at 700 °C to provide phase equilibria data for the Cu–Ni–Si system.

2. Experimental procedure

Thirty ternary alloys were prepared in this work using raw materials of Cu(99.99 wt.%), Ni(99.99 wt.%) and Si(99.9999 wt.%) blocks, with their nominal compositions presented in Table 2 and plotted in Fig. 1. The alloys with weight between 1 and 2 g were prepared by arc melting under high purity argon atmosphere. Encapsulated in evacuated silica tubes with a residual argon pressure of 10^{-3} bar, the alloys were annealed at 700 °C for 30 days or more, followed by water quenching. Since the weight loss of each alloy after arc melting was less than 0.5 wt.%, the alloys were not subjected to chemical analysis.

The phase identification was conducted by means of XRD using Cu Kα radiation. After standard metallographic preparation, the alloys were investigated using optical microscopy (Leica DMLP, Germany) and scanning electron microscopy (SEM) equipped with energy dispersive X-ray spectroscopy (EDS) (JSM-6360LV, JEOL, Japan) to determine tie-lines or tie-triangle data. It was found that the nominal

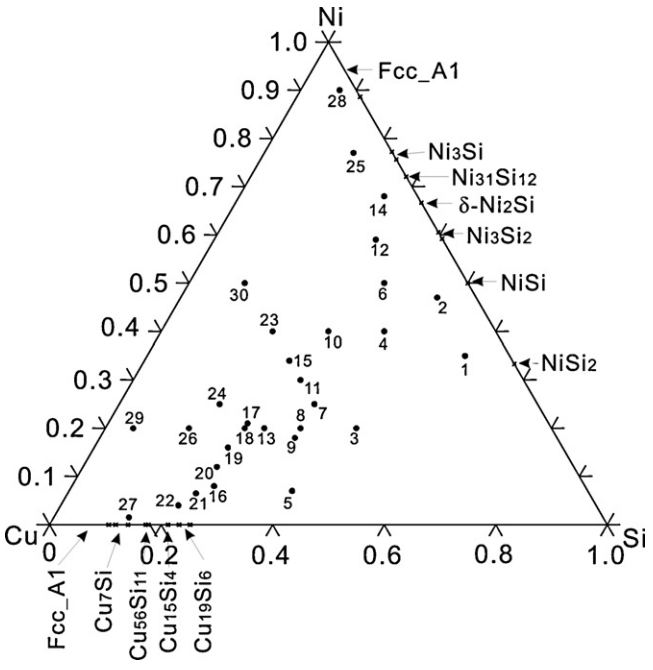

Fig. 1. Nominal alloy composition.

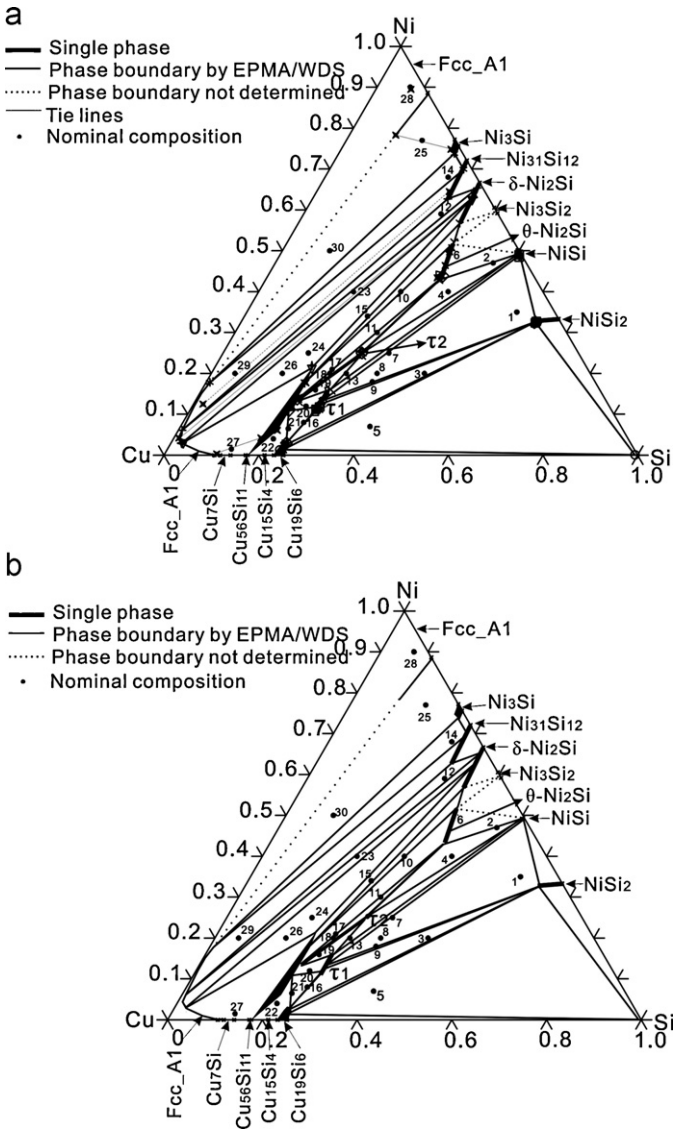

Fig. 2. Experimental isothermal section at 700 °C (a) with EPMA results; (b) without EPMA results.

Table 2
Summary of the identified phases, their compositions and lattice parameters for the Cu–Ni–Si alloys annealed at 700 °C.

No.	Nominal composition (at.%)			Phase[a]	Phase composition[b] (at.%)			Lattice parameters (Å)[b]		
	Cu	Ni	Si		Cu	Ni	Si	*a*	*b*	*c*
1	8	35	57	τ_1	61.2	11.8	27	–		
				$NiSi_2$	5	32.7	62.3	5.405(1)		
				NiSi	0.5	49	50.5	5.183(1)	3.343(2)	5.622(2)
2	7	47	46	NiSi	0.2	49.5	50.3	5.188(1)	3.341(1)	5.622(1)
				θ-Ni_2Si	17.4	46.4	36.2	3.889(1)		4.988(2)
3[c]	35	20	45	τ_1	59.8	13.3	26.9	–		
				$Cu_{19}Si_6$	73	2.7	24.3	6.0156(9)	6.337(9)	4.277(7)
				$NiSi_2$	5.8	32	62.2	5.4021(5)		
4[c]	20	40	40	τ_2	45	25.5	29.5	–		
				NiSi	0.7	48.5	50.8	5.184(1)	3.342(2)	5.625(2)
				θ-Ni_2Si	19.5	44.5	36	–		
5	53	7	40	Si	0.5	0.1	99.4	5.439(1)		
				$NiSi_2$	4.9	32.6	62.5	5.407(1)		
				$Cu_{19}Si_6$	74.9	1.3	23.8	6.03(1)	6.323(7)	4.288(5)
6	15	50	35	θ-Ni_2Si	14.8	49.7	35.5	3.897(3)		4.992(2)
7[c]	40	25	35	τ_1	61.5	11.2	27.3	–		
				NiSi	0.6	49	50.4	5.199(5)	3.347(5)	5.640(6)
8[c]	45	20	35	τ_1	62.3	11.2	26.5	–		
				$NiSi_2$	5.4	32.4	62.2	5.408(1)		
				NiSi	0.8	48.4	50.8	5.198(2)	3.347(2)	5.629(3)
9	47	18	35	τ_1	63	10.4	26.6	–		
				$NiSi_2$	5.2	32.6	62.2	5.4043(8)		
				NiSi	0.5	48.9	50.6	5.186(3)	3.349(5)	5.619(7)
10[c]	30	40	30	$Cu_{56}Si_{11}$	61.2	17.7	21.1	6.1771(6)		
				θ-Ni_2Si	13.9	50.7	35.4	3.895(2)		4.990(2)
11[c]	40	30	30	τ_2	45.3	25.3	29.4	–		
				$Cu_{56}Si_{11}$	64.6	13.9	21.5	6.189(1)		
				θ-Ni_2Si	20.3	43	36.7	3.884(3)		4.991(5)
12	12	59	29	δ-Ni_2Si	1.2	65.3	33.5	7.074(2)	5.005(1)	3.7351(9)
				$Ni_{31}Si_{12}$	8.7	62.7	28.6	–		
				Fcc_A1	93.1	6.1	0.8	3.6171(5)		
13	51.5	20	28.5	τ_1	57.7	15.7	26.6	–		
				τ_2	46.7	24.6	28.7	–		
				NiSi	0.4	49.6	50	–		
14	6	68	26	$Ni_{31}Si_{12}$	1.8	69.9	28.3	6.688(7)		12.319(7)
				Ni_3Si	1.8	73.8	24.4	3.5107(4)		
				Fcc_A1	81.4	17.8	0.8	3.6051(6)		
15[c]	40	34	26	$Cu_{56}Si_{11}$	61.5	17.6	20.9	6.176(1)		
				δ-Ni_2Si	9.2	56.7	34.1	–		
				θ-Ni_2Si	12.7	52.1	35.2	3.896(4)		4.991(7)
16	66.5	8	25.5	τ_1	61.4	12	26.6	–		
				$Cu_{19}Si_6$	72.9	3	24.1	6.0258(8)	6.3298(6)	4.2771(4)
17	54	21	25	$Cu_{56}Si_{11}$	65.2	13.6	21.2	6.1837(4)		
				θ-Ni_2Si	20.6	43.4	36	3.893(3)		4.989(6)
18[c]	55	20	25	τ_2	45.7	25	29.3	–		
				$Cu_{56}Si_{11}$	65	13.7	21.3	6.1841(6)		
				θ-Ni_2Si	19.2	43.8	37	3.880(3)		4.995(5)
19[c]	60	16	24	τ_1	56.8	16.1	27.1	–		
				τ_2	46.1	24.6	29.3	–		
				$Cu_{56}Si_{11}$	65.1	13.3	21.6	6.1878(8)		
20	64	12	24	τ_1	60	13.2	26.8	–		
				$Cu_{56}Si_{11}$	67	11.8	21.2	6.192(1)		
21	70.5	6.5	23	τ_1	61.3	11.9	26.8	–		
				$Cu_{19}Si_6$	72.6	3	24.4	6.023(4)	6.332(2)	4.271(2)
				$Cu_{56}Si_{11}$	68.2	10.9	20.9	6.1932(4)		
22[c]	74.9	4	21.1	$Cu_{19}Si_6$	74.1	1.3	24.6	6.011(5)	6.322(3)	4.276(3)
				$Cu_{56}Si_{11}$	73	6.1	20.9	6.2000(3)		
23[c]	40	40	20	δ-Ni_2Si	2.6	63.7	33.7	7.082(5)	5.004(3)	3.744(2)
				Fcc_A1	94.7	4.2	1.1	3.616(2)		
24	57	25	18	$Cu_{56}Si_{11}$	57.8	21.9	20.3	6.167(1)		
				δ-Ni_2Si	3.3	63	33.7	7.065(5)	5.015(3)	3.742(2)
				Fcc_A1	94.8	2.9	2.3	3.619(1)		
25	7	77	16	Ni_3Si	2	74.8	23.2	3.521(1)		
				Fcc_A1	11.9	78.3	9.8	3.5345(6)		
26	65	20	15	$Cu_{56}Si_{11}$	58.1	21.3	20.6	6.1598(8)		
				δ-Ni_2Si	3.6	62.6	33.8	7.068(2)	5.003(1)	3.7297(8)
				Fcc_A1	94.4	3.1	2.5	3.614(2)		
27	85	1.5	13.5	$Cu_{56}Si_{11}$	77.4	4.2	18.4	6.216(1)		
				Fcc_A1	88.7	0.3	11	3.6252(3)		
28	3	90	7	Fcc_A1	3.1	89.5	7.4	3.525(1)		
29[c]	75	20	5	$Ni_{31}Si_{12}$	7.5	64.5	28	6.694(4)		12.30(1)
				Fcc_A1	85.5	12.5	2	3.609(2)		

Table 2 (*Continued*)

No.	Nominal composition (at.%)			Phase[a]	Phase composition[b] (at.%)			Lattice parameters (Å)[b]		
	Cu	Ni	Si		Cu	Ni	Si	*a*	*b*	*c*
30[c,d]	40	50	10	Ni_3Si	3	72.7	24.3	–		
				Fcc_A1	46.6	46.3	7.1	–		

[a] The determination of τ_1 and τ_2 depends on the comparison between the XRD patterns of the corresponding alloys and EPMA results because there are no standard XRD patterns for τ_1 and τ_2.
[b] For θ-Ni_2Si and $Ni_{31}Si_{12}$ phases, $\alpha=\beta=90^\circ$, $\gamma=120^\circ$, for other phases, $\alpha=\beta=\gamma=90^\circ$.
[c] These alloys were annealed for 30 days at 700 °C while the others were annealed for 80 days.
[d] The result of alloy 30 is deleted in constructing the phase diagram since the microstructure shows the alloy does not reach equilibrium.

compositions of some alloys, whose weight loss after arc melting was negligible, were not in the tie-triangle measured by SEM/EDS. Then, all the alloys were further examined by electron probe microanalysis equipped with wave dispersive X-ray spectroscopy (EPMA/WDS) (JXA-8100, JEOL, Japan) to acquire more accurate data.

3. Experimental result and discussion

The identified phases, their compositions and lattice parameters in the alloys are presented in Table 2. Fig. 2 shows the measured isothermal section at 700 °C. Sixteen alloys are in three-phase regions, so 12 tie-triangles were determined: $Cu_{19}Si_6$+$NiSi_2$+Si, $Cu_{19}Si_6$+τ_1+$NiSi_2$, τ_1+NiSi+$NiSi_2$, $Cu_{56}Si_{11}$+τ_1+$Cu_{19}Si_6$, τ_2+τ_1+NiSi, $Cu_{56}Si_{11}$+τ_2+τ_1, τ_2+θ-Ni_2Si+NiSi, $Cu_{56}Si_{11}$+θ-Ni_2Si+τ_2, $Cu_{56}Si_{11}$+δ-Ni_2Si+θ-Ni_2Si, Fcc_A1+δ-Ni_2Si+$Cu_{56}Si_{11}$, Fcc_A1+$Ni_{31}Si_{12}$+δ-Ni_2Si, Fcc_A1+Ni_3Si+$Ni_{31}Si_{12}$. Figs. 3 and 4 show the XRD patterns and microstructure of representative alloys.

The XRD pattern of alloy 5($Cu_{53}Ni_7Si_{40}$) in Fig. 3a shows this alloy is in $Cu_{19}Si_6$+$NiSi_2$+Si three-phase region, which is in agreement with the microstructure and EPMA result presented in Fig. 4a. Alloys 3($Cu_{35}Ni_{20}Si_{45}$) and 21($Cu_{70.5}Ni_{6.5}Si_{23}$) determine the three-phase triangles of $Cu_{19}Si_6$+τ_1+$NiSi_2$ and $Cu_{56}Si_{11}$+$Cu_{19}Si_6$+τ_1, respectively. Alloys 1($Cu_8Ni_{35}Si_{57}$), 8($Cu_{45}Ni_{20}Si_{35}$) and 9($Cu_{47}Ni_{18}Si_{35}$) are all in the τ_1+NiSi+$NiSi_2$ three-phase region. Alloys 7($Cu_{40}Ni_{25}Si_{35}$), 16($Cu_{66.5}Ni_8Si_{25.5}$), 20($Cu_{64}Ni_{12}Si_{24}$) and 22($Cu_{74.9}Ni_4Si_{21.1}$), which locate in two-phase regions, further confirm the determined tie-triangles. Alloys 13($Cu_{51.5}Ni_{20}Si_{28.5}$), 4($Cu_{20}Ni_{40}Si_{40}$), 19($Cu_{60}Ni_{16}Si_{24}$), 11($Cu_{40}Ni_{30}Si_{30}$) and 18($Cu_{55}Ni_{20}Si_{25}$) determine the three-phase regions of τ_2+τ_1+NiSi, τ_2+θ-Ni_2Si+NiSi, $Cu_{56}Si_{11}$+τ_2+τ_1 and $Cu_{56}Si_{11}$+θ-Ni_2Si+τ_2, respectively. Fig. 4b and c present the microstructure of alloys 9($Cu_{47}Ni_{18}Si_{35}$) and 13($Cu_{51.5}Ni_{20}Si_{28.5}$) respectively. All the analyses on these alloys reveal two ternary compounds τ_1 and τ_2. The τ_1 phase has previously been observed by Okamoto [22] below 850 °C around $Cu_{60.9-66.3}Ni_{9.9-11.2}Si_{23.4-28.3}$. The present EPMA results show that its homogeneity range is $Cu_{56.8-63}Ni_{10.4-16.1}Si_{26.6-27.3}$ at 700 °C. The ternary compound τ_2 is observed in this work for the first time. The composition of this phase is determined to be almost constant $Cu_{45.8}Ni_{25}Si_{29.2}$ from EPMA analyses on alloys 4, 11, 13, 18 and 19. It should be mentioned that there are no standard XRD patterns for τ_1 and τ_2. The determination of these two phases depends on the comparison between the XRD patterns of the corresponding alloys and EPMA results.

The θ-Ni_2Si phase exists only above 820 °C in the binary Ni–Si system, but can be stabilized down to 500 °C in the Cu–Ni–Si ternary system by dissolving Cu, as observed by Sokolovskaya et al. [28]

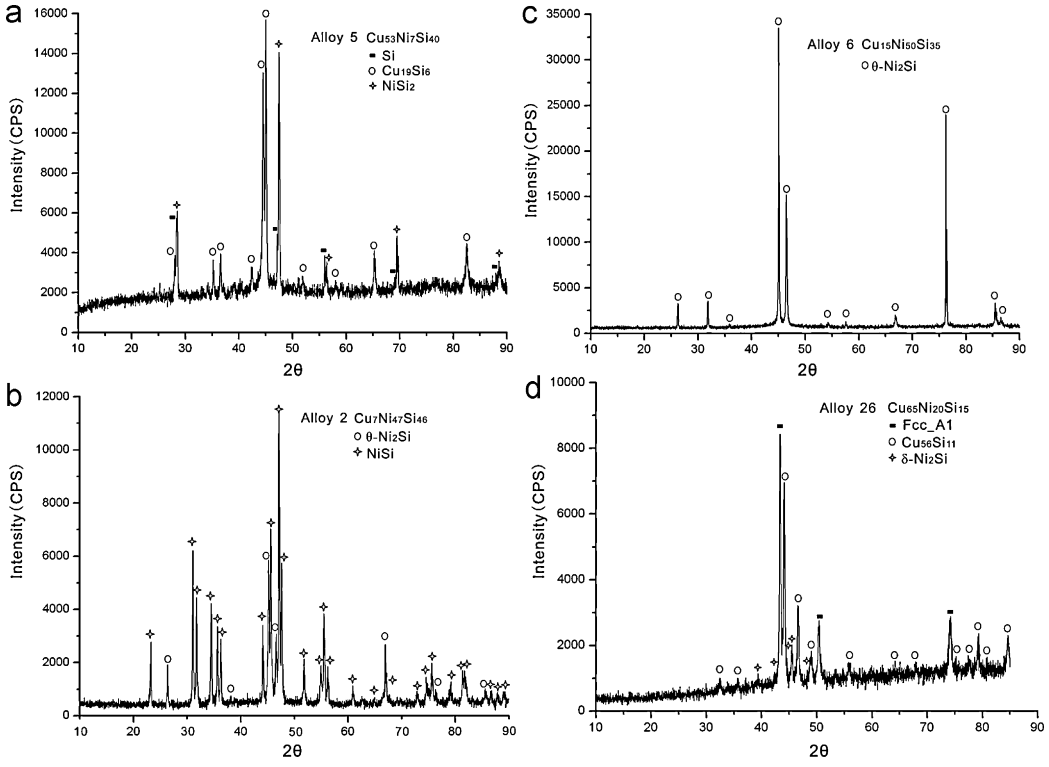

Fig. 3. XRD patterns for alloys (a) 5($Cu_{53}Ni_7Si_{40}$); (b) 2($Cu_7Ni_{47}Si_{46}$); (c) 6($Cu_{15}Ni_{50}Si_{35}$); (d) 26 ($Cu_{65}Ni_{20}Si_{15}$).

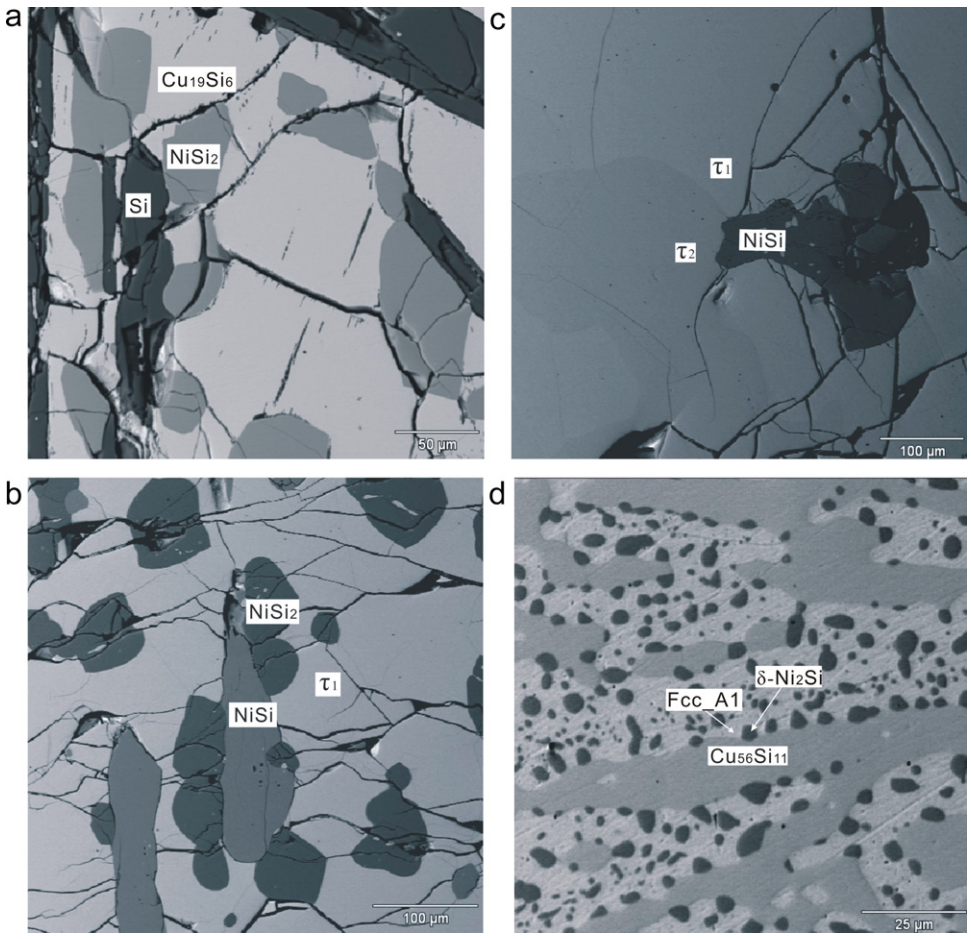

Fig. 4. Back scattered electron images of alloys (a) 5($Cu_{53}Ni_7Si_{40}$); (b) 9($Cu_{47}Ni_{18}Si_{35}$); (c) 13($Cu_{51.5}Ni_{20}Si_{28.5}$); (d) 26 ($Cu_{65}Ni_{20}Si_{15}$).

using XRD. It was corroborated by the present experimental observation, for example, the XRD identification of this phase in the alloys 2($Cu_7Ni_{47}Si_{46}$) and 6($Cu_{15}Ni_{50}Si_{35}$) equilibrated at 700 °C shown in Fig. 3b and c. By substituting Cu for Ni, the θ-Ni_2Si phase can extend into the ternary system with a solubility of Cu varying from 12.7 to 20.6 at.% at 700 °C, together with a Si content varying from 35.2 to 37 at.%, which indicates a slight substitution of Si for Ni. The θ-Ni_2Si phase was identified to be equilibrated with NiSi (alloy 2), τ_2 (alloys 4, 11, and 18), $Cu_{56}Si_{11}$ (alloys 10, 11, 15, 17 and 18), and δ-Ni_2Si (alloy 15).

Alloys 14($Cu_6Ni_{68}Si_{26}$) and 12($Cu_{12}Ni_{59}Si_{29}$) are in three-phase regions Fcc_A1+Ni_3Si+$Ni_{31}Si_{12}$ and Fcc_A1+$Ni_{31}Si_{12}$+δ-Ni_2Si, respectively. Alloys 24($Cu_{57}Ni_{25}Si_{18}$) and 26($Cu_{65}Ni_{20}Si_{15}$) are in the same three-phase region, Fcc_A1+δ-Ni_2Si+$Cu_{56}Si_{11}$. Figs. 3d and 4d show the XRD pattern and microstructure of alloy 26($Cu_{65}Ni_{20}Si_{15}$), respectively. Alloys 29($Cu_{75}Ni_{20}Si_5$) and 23($Cu_{40}Ni_{40}Si_{20}$)) are in two-phase $Ni_{31}Si_{12}$+Fcc_A1 and Fcc_A1+δ-Ni_2Si regions. The tie-triangles determined by these alloys show agreement with the results of Sokolovskaya et al. [28] at 500 °C. The EPMA result shows that in the copper rich corner, the solubility of Si is decreased to minimum, which means a little addition of Si can cause the precipitation of δ-Ni_2Si or $Ni_{31}Si_{12}$ compounds from the Fcc_A1 matrix. This trend can further demonstrate the mechanism of the age-hardening of the Corson alloy although the current experimental temperature is higher than the optimal heat treatment temperature of 450–500 °C.

The $Cu_{56}Si_{11}$ can dissolve a large amount of Ni up to 21.9 at.% mainly by substituting Ni for Cu. At the same time, the Si content also varies slightly with increasing the Ni content. This trend was previously observed at 500 °C [28]. Fig. 5 shows the lattice parameters of $Cu_{56}Si_{11}$ phase versus Ni content while the Si content is within 21 ± 0.7 at.%. The lattice parameter decreases as Ni content increases. Such an increase can be explained by the substitution of large Cu atom with smaller Ni atom in $Cu_{56}Si_{11}$ phase. $Cu_{19}Si_6$ can dissolve 3 at.% Ni and the Si content remains about 24 at.%. Less than 1 at.% Cu is observed in NiSi compound. $NiSi_2$ can dissolve Cu

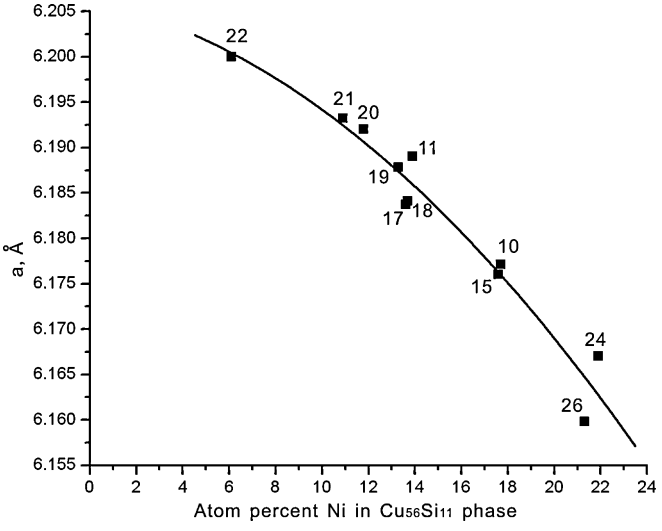

Fig. 5. Lattice parameters of $Cu_{56}Si_{11}$ phase versus Ni content.

to 5.8 at.%, but Cu substitutes more Si than Ni. In contrast, Cu substitutes much Ni to 9.2 at.% Ni and 8.6 at.% Ni in δ-Ni_2Si and $Ni_{31}Si_{12}$ respectively, but the Si content remains nearly constant.

4. Conclusion

The isothermal section at 700 °C was determined by XRD, SEM/EDS and EPMA. The existence of the ternary compound τ_1 is confirmed and it shows a limited homogeneity. A new ternary compound τ_2 is observed and nearly no homogeneity range was observed. It is corroborated that the θ-Ni_2Si phase can be stabilized by substituting Cu for Ni at low temperatures in the Cu–Ni–Si system. Significant or noticeable solubilities of the third element in the ternary system were observed in the binary compounds $Cu_{56}Si_{11}$, $Ni_{31}Si_{12}$, δ-Ni_2Si and θ-Ni_2Si at 700 °C.

Acknowledgements

The financial support from the National Basic Research Program of China (Grant No. 2011CB610401) and the National Natural Science Foundation of China (Grant Nos. 50831007, 51021063 and 50971135) is greatly acknowledged. Mr. Shu Zheng at State Key Lab of Geological Processes and Mineral Resources in China University of Geosciences is acknowledged for help on EPMA analysis.

References

[1] M.G. Corson, Z. Metallkd. 19 (1927) 370–371.
[2] M.G. Corson, Iron Age 119 (1927) 421–424.
[3] M.G. Corson, Rev. Met. 27 (1930) 194–213.
[4] M.G. Corson, Rev. Met. 27 (1930) 265–281.
[5] N. Era, K. Fukamachi, J. Jpn. Res. Inst. Adv. Copper-Base Mater. Technol. 44 (2005) 136–139.
[6] A. Nishimoto, T. Kamimura, T. Maruyama, K. Nakao, K. Akamatsu, T. Kobayashi, J. Jpn. Res. Inst. Adv. Copper-Base Mater. Technol. 45 (2006) 31–36.
[7] G. Hagino, H. Eguchi, Y. Takayama, H. Kato, Mater. Sci. Forum 654–656 (2010) 2568–2571.
[8] http://www.nmm.jx-group.co.jp/english/products/01_atsuen/03cunisi.htm.
[9] M.D. Teplitskii, A.K. Nikolaev, N.I. Revina, V.M. Rozenberg, Fiz. Met. Metalloved. 40 (1975) 1240–1243.
[10] Y.G. Kim, T.Y. Seong, J.H. Han, J. Mater. Sci. 21 (1986) 1357–1362.
[11] S.A. Lockyer, F.W. Noble, J. Mater. Sci. 29 (1994) 218–226.
[12] N.F. Lashko, K.P. Sorokina, A.N. Gorbunov, Metalloved. Term. Obrab. Met. 6 (1966) 48–49.
[13] E. Jänecke, Brief Handbook of Alloys, Winter, Heidelberg, 1949.
[14] Y.A. Chang, J.P. Neumann, A. Mikula, D. Goldberg, INCRA Monograph Series 6 Phase Diagrams and Thermodynamic Properties of Ternary Copper–Metal System, NSRD, Washington, 1979.
[15] M.E. Drits, N.R. Bochvar, L.S. Guzei, E.V. Lysova, N. Padezhnova, L.L. Rokhlin, N.I. Turkina, Binary and Multicomponent Copper-Base Systems, Nauka, Moscow, 1979.
[16] K.C. Hari Kumar, A. Kussmaul, H.L. Lukas, G. Effenberg, Cu–Ni–Si, in: G. Effenberg, S. Ilyenko (Eds.), Materials – The Landolt-Börnstein Database, Springer (http://www.springermaterials.com), doi:10.1007/978-3-540-47000-7_33.
[17] E. Crepaz, Metall. Ital. 23 (1931) 711–716.
[18] D.G. Jones, L.B. Pfeil, W.T. Griffiths, J. Inst. Met. 46 (1931) 423–442.
[19] C.H.M. Jenkins, E.H. Bucknell, J. Inst. Met. 57 (1935) 141–189.
[20] M. Okamoto, J. Jpn. Inst. Met. 2 (1938) 211–232.
[21] M. Okamoto, J. Jpn. Inst. Met. 3 (1939) 336–348.
[22] M. Okamoto, J. Jpn. Inst. Met. 3 (1939) 365–402.
[23] M. Okamoto, J. Jpn. Inst. Met. 3 (1939) 411–420.
[24] I.I. Novikov, L.I. Dautova, Zh. Neorg. Khim. 2 (1957) 2766–2770.
[25] I.I. Novikov, L.I. Dautova, Trudy Inst. Yadernoi Fiz., Akad. Nauk Kazakh. SSR 1 (1958) 274–281.
[26] N.F. Lashko, K.P. Sorokina, Zh. Neorg. Khim. 4 (1959) 1613–1615.
[27] E.M. Sokolovskaya, O.I. Chechernikova, E.I. Gladyshevskii, O.I. Bodak, Vestn. Mosk. Univ., Ser. 2: Khim. 12 (1971) 446–449.
[28] E.M. Sokolovskaya, O.I. Chechernikova, E.I. Gladyshevskii, O.I. Bodak, Izv. Akad. Nauk SSSR, Metally 6 (1973) 192–196.
[29] O.I. Chechernikova, E.M. Sokolovskaya, L.S. Guzei, Vestn. Mosk. Univ., Ser. 2: Khim. 13 (1972) 486–489.
[30] E. Lugscheider, Proc. 5th Int. Conf. Therm. Anal. (ICTA 5) 9 (1977) 8–101.
[31] V. Witusiewicz, I. Arpshofen, H. Siefert, F. Sommer, F. Aldinger, Z. Metallkd. 91 (2000) 128–142.
[32] T.B. Massalski, Binary Alloy Phase Diagrams, second ed., ASM International, Metals Park, OH, 1986.
[33] H.E. Swanson, E. Tatge, Natl. Bur. Stand. (U.S.) Circ. 539 (1953) 1–95.
[34] M.C. Morris, H.F. McMurdie, Natl. Bur. Stand. (U.S.) Monogr. 25 (1976) 1–109.
[35] Y. Oya, T. Suzuki, Z. Metallkd. 74 (1983) 21–24.
[36] G.S. Saini, L.D. Calvert, J.B. Taylor, Can. J. Chem. 42 (1964) 1511–1517.
[37] PDF2004, International Centre for Diffraction Data, PA, USA.
[38] G. Pilstrom, Acta Chem. Scand. 15 (1961) 893–902.
[39] A. Osawa, M. Okamoto, Sci. Rep. Fac. Sci., Kyushu Univ., Geol. 27 (1939) 326–347.
[40] K. Toman, B. Panenske, V. Odolena, Acta Crystallogr. 4 (1951) 462–464.
[41] K. Schubert, H. Pfisterer, Z. Metallkd. 41 (1950) 433–441.
[42] S. Arrhenius, A. Westgren, Z. Phys. Chem. 14 (1931) 66–79.
[43] F.R. Morral, A. Westgren, Ark. Kemi, Mineral. Geol. 11B (1934) 1–6.